





Article

Mesoporous Layered Double Hydroxides: Synthesis for High Effective Uranium Ions Sorption from Seawater and Salt Solutions on Nanocomposite Functional Materials

Valeria A. Balybina ¹, Artur N. Dran'kov ¹ , Oleg O. Shichalin ^{1,*} , Natalia Yu. Savel'eva ¹, Nadezhda G. Kokorina ¹, Zhanna C. Kuular ¹, Nikita P. Ivanov ¹, Svetlana G. Krasitskaya ¹, Andrei I. Ivanets ² , and Evgeniy K. Papynov ¹ 

¹ Nuclear Technology Laboratory, Department of Nuclear Technology, Institute of High Technologies and Advanced Materials, Far Eastern Federal University, 10 Ajax Bay, Russky Island, Vladivostok 690922, Russia; balybina.va@dvmfu.ru (V.A.B.); artur.drancov@gmail.com (A.N.D.); ivanov.np@dvmfu.ru (N.P.I.); papynov@mail.ru (E.K.P.)

² Institute of General and Inorganic Chemistry of National Academy of Sciences of Belarus, Surganova St. 9/1, 220072 Minsk, Belarus; andreiivanets@yandex.by

* Correspondence: oleg_shich@mail.ru

Abstract: A series of sorption materials based on layered double hydroxides (Co-Fe LDH, Ni-Fe LDH, and Zn-Ti LDH) were obtained by a facile and environmentally friendly method of coprecipitation. A low particle size of no more than 10 μm was achieved. The use of transition metals makes it possible to obtain compounds that are mechanically and chemically stable in aggressive environments. XRD analysis revealed that the compounds have a highly organized crystalline structure. Using SEM, it was determined that Co-Fe LDH and Ni-Fe LDH had a loose, highly dispersed surface structure, while Zn-Ti LDH had a monolithic surface structure. U(VI) adsorption on the obtained materials in solutions containing Na_2CO_3 , Na_2SO_4 , KNO_3 , NaCl , K_3PO_4 , and NaHCO_3 , was studied in batch mode. The degree of purification in the presence of these salts reached 99.9%, while the distribution coefficient K_d reached 10^5 mL/g. Sorption capacity q_{max} and equilibrium adsorption constants K_f and K_L for U(VI) adsorption in batch mode (for 24 h) from distilled and seawater were determined using the Freundlich and Langmuir equations. The highest sorption capacity of 101.6 mg/g in seawater and 114.1 mg/g in distilled water was registered for Co-Fe-LDH. The presence of competing ions in seawater can reduce sorption efficiency by up to 40%. The provided research allowed us to conclude that the obtained materials, Co-Fe LDH, Ni-Fe LDH, and Zn-Ti LDH are promising for the sorption removal of U(VI) from aqueous media of medium salinity.

Keywords: inorganic sorbents; nanocomposite functional materials; sorption; layered double hydroxides; uranium (VI); seawater



Citation: Balybina, V.A.; Dran'kov, A.N.; Shichalin, O.O.; Savel'eva, N.Y.; Kokorina, N.G.; Kuular, Z.C.; Ivanov, N.P.; Krasitskaya, S.G.; Ivanets, A.I.; Papynov, E.K. Mesoporous Layered Double Hydroxides: Synthesis for High Effective Uranium Ions Sorption from Seawater and Salt Solutions on Nanocomposite Functional Materials. *J. Compos. Sci.* **2023**, *7*, 458. <https://doi.org/10.3390/jcs7110458>

Academic Editor: Aleksey A. Vedyagin

Received: 18 September 2023

Revised: 14 October 2023

Accepted: 27 October 2023

Published: 3 November 2023



Copyright: © 2023 by the authors. Licensee MDPI, Basel, Switzerland. This article is an open access article distributed under the terms and conditions of the Creative Commons Attribution (CC BY) license (<https://creativecommons.org/licenses/by/4.0/>).

1. Introduction

Uranium is a highly toxic radioactive element that is widely used in various fields such as chemical, energy, aerospace, metallurgical, and others [1]. Uranium fuel is the most important raw material for nuclear power, providing 10% of all electricity produced in the world [2]. In this regard, uranium reserves may be a limiting factor in the development of nuclear energy. The process of uranium mining and the use of nuclear energy is generating large amounts of wastewater and radioactive waste containing U(VI) in the form of hexavalent uranyl cations (UO_2^{2+}) [3]. Therefore, the removal of soluble uranium from radiation-contaminated waters for the purpose of its subsequent use in technological processes of nuclear energy is becoming an increasingly urgent task.

Uranium can be removed from liquid media using promising sorption materials based on layered double hydroxides (LDH). These sorbents have a unique layered crystal

structure, an abundance of active sorption sites, high selectivity, and a high specific surface area. These advantages allow LDH to effectively adsorb heavy metals, including uranyl ions, on its surface [4,5].

LDH or other hydrotalcite-like compounds have a distinct layered structure and general formula $[M^{2+}_{1-x}M^{3+}_x(OH)_2]^{x+}(A^{n-})_{x/n} \cdot mH_2O$, where M^{2+} —divalent metal, M^{3+} —trivalent metal, located in octahedral positions of brucite-like layers, and A^{n-} —anion, compensating the positive charge of brucite-like layers [6]. The formation of the hydroxide phase occurs provided that the x value lies in the range of 0.2–0.4, and the radii of the cations forming brucite-like layers do not differ by more than 1.5 times. Anions, when interacting with these compounds, can adsorb on their outer surface and penetrate the interlayer space due to anion exchange or LDH reconstruction (“memory effect”) [7,8]. The structural features of LDHs and the variety of cations included in their composition determine various ion exchange, sorption, catalytic, and other properties. For example, the synthesis of LDHs with magnetic properties, which can significantly simplify the process of extracting spent sorbents from aqueous media, is carried out through the simultaneous introduction of iron and cobalt cations into the system [9].

Several studies carried out using synchrotron radiation (XANES and EXAFS methods) give us knowledge about the main mechanisms of uranium adsorption on the surface of LDH [10–15].

The authors of the study [13] found that these mechanisms include: (i) complexation occurring between UO_2^{2+} and ions contained in the interlayer space of the LDH and subsequent intercalation of electroneutral complexes into the interlayer space; (ii) complexation with carbonate ions located in the interlayer space of the LDH and subsequent intercalation of electronegative complexes (such as $UO_2(CO_3)_2^{2-}$) into the interlayer space; (iii) surface precipitation of uranium in the form of $UO_2(OH)_2$. The specific type of adsorption mechanism depends on many parameters, mainly the concentration of uranyl ions.

According to another study [14], the main mechanisms of uranium adsorption on LDH are surface complexation occurring through the deprotonation of Me-OH functional groups and ion exchange of negatively charged uranium complexes (mainly carbonate) with ions (Cl^- , NO_3^-) in the interlayer space of the LDH.

The study [15] showed that the adsorption of uranium on Mg-Al-LDH can occur as a consequence of (i) precipitation of uranyl hydroxide $UO_2(OH)_2$ and similar basic uranium compounds on the surface of the LDH; and (ii) surface complexation with the formation of complexes such as $Mg(UO_2(CO_3)_3)^{2-}$ and $UO_2(CO_3)_3^{4-}$ (Mg^{2+} was a component of the Mg-Al-LDH crystal lattice). At the same time, at high pH, mainly the precipitation of basic uranium compounds on the surface of the LDH was observed.

The results of another study showed that the mechanisms responsible for the adsorption of uranium on LDH are inner-sphere complexation (at $pH > 5$) and cation exchange (at $pH < 4$) [12].

The authors [11] showed that the adsorption of uranium on Ca-Al-LDH and Ni-Al-LDH samples modified with glycerol proceeds according to a slightly different mechanism. Ca-Al-LDH has been shown to be capable of extracting uranium via outer-sphere surface complexation and electrostatic interactions, while Ni-Al-LDH extracts uranium through inner-sphere surface complexation and electrostatic interactions.

Thus, based on the obtained literature data based on the use of XANES and EXAFS methods to study the mechanisms of uranium adsorption on LDH, it can be assumed that the specific adsorption mechanism depends on many factors, such as pH, uranium concentration, content and type of interfering ions, the type of ions in the interlayer space of the LDH, and even the type of metals that make up the crystalline lattice of the LDH. The main mechanisms of adsorption, the occurrence of which is confirmed by most studies, are (i) surface complexation, which can be either outer-sphere or inner-sphere; and (ii) surface precipitation of uranium in the form of uranyl hydroxide (at high pH values).

Zn-Al LDH, containing EDTA, DTPA, and HMDTA, demonstrates a high sorption capacity for uranyl ions in the presence of carbonate ions for the process of the extraction of U(VI) in the interlayer space [16]. The sorbent based on Mg-Al double oxide was synthesized by calcination of Mg-Al double hydroxide synthesized by the homogeneous precipitation method. The proposed material can effectively remove uranyl ions due to complexation on the surface and the “memory effect”, which results in the reconstruction of the layered structure of heat-treated forms of LDH [5,17]. There is a similar method for obtaining sorption material for the extraction of U(VI) based on U(VI) Mg-Fe LDH, which was obtained by coprecipitation and thermally treated in an air atmosphere. Using this method, Mg-Fe LDH and Zn-Al LDH were obtained, which have a high sorption capacity for uranyl ions of 201.09 mg/g [18]. However, the presented sorption materials are characterized by low mechanical resistance and are prone to peptization during sorption experiments, which does not imply the use of these materials in dynamic modes.

To increase the sorption activity of LDH compared to analogues, a hydrothermal synthesis method is proposed, which includes the preliminary stages of obtaining carbon spheres and coating them with Ni-Al LDH [19]. In the article [20], a similar synthesis is implemented, where SiO₂ with AlOOH are used as microspheres. The study [21] proposed the preparation of three-dimensional hydroxyapatite materials based on Mg-Fe LDH (Mg-Fe-HAP) using ultrasonic synthesis, hydrothermal synthesis, and coprecipitation methods. HAP was obtained by the coprecipitation method and Mg-Fe LDH by the hydrothermal method. The resulting materials demonstrate a high sorption capacity for uranyl ions of 845.16 mg/g. However, the identified disadvantages of such complex sorbents were their low mechanical stability in acidic environments and the low degree of uranium recovery in alkaline and carbonate solutions.

The main negative effect on U(VI) adsorption is exerted by co-existing CO₃²⁻. This is due to the existence of many uranyl carbonate forms (such as UO₂CO₃ (aq), UO₂(CO₃)₂²⁻, and UO₂(CO₃)₃⁴⁻). At high concentrations, they cause a process of electrostatic repulsion between the surface of the adsorbent and UO₂²⁺ [22–25]. Due to its ability to adsorb radionuclide ions through surface deposition, ion exchange, and isomorphic substitution mechanisms, LDH is considered an effective material for radioactive wastewater treatment [26]. However, the adsorption efficiency of pollutants onto LDH may be limited due to the lack of surface functional groups.

To avoid the dissolution of LDH and the removal of metal ions that make up its crystal lattice into the filtrate, several authors have proposed a regeneration method using Na₂CO₃ or NaHCO₃ solutions, which make it possible to remove intercalated forms of uranium from the interlayer space of LDH. The study [20] showed that at a Na₂CO₃ concentration of 0.5 mol/L or more, the desorption efficiency is 80%. The authors [27] showed that after four cycles of adsorption–desorption with NaHCO₃, the removal ratio of uranium by LDH was maintained at 90.27%. The article [28] compares the effectiveness of NaOH, Na₂CO₃, and EDTA for the regeneration of adsorbed uranium, and shows that the most effective desorption method is the treatment of Na₂CO₃.

LDH of transition metals (Co-Fe LDH, Ni-Fe LDH, and Zn-Ti LDH) can be used as efficient sorption materials for U(VI) removal due to the increased chemical activity of their hydroxyl functional groups. The synthesis of such materials can be realized by a facile and environmentally friendly method of coprecipitation.

The purpose of the research is to obtain layered double hydroxides (LDH) based on transition metals (Co-Fe, Ni-Fe, and Zn-Ti) using a simple coprecipitation method. The use of transition metals makes it possible to obtain compounds that are mechanically and chemically stable in aggressive environments while maintaining high activity in liquid media redox reactions. In addition, a study and comparison of the physico-chemical properties of the obtained materials and their sorption properties for U(VI) were carried out.

The novelty of the research lies in the use of new combinations of metals to create layered double hydroxides, as well as in the study of their sorption efficiency in various solutions, such as seawater and solutions containing various salts.

2. Experimental

2.1. Materials and Reagents

The following reagents were used: cobalt chloride hexahydrate ($\text{CoCl}_2 \cdot 6\text{H}_2\text{O}$), iron chloride hexahydrate ($\text{FeCl}_3 \cdot 6\text{H}_2\text{O}$), sodium hydroxide (NaOH), sodium carbonate (Na_2CO_3), nickel chloride hexahydrate ($\text{NiCl}_2 \cdot 6\text{H}_2\text{O}$), iron chloride hexahydrate ($\text{FeCl}_3 \cdot 6\text{H}_2\text{O}$), zinc chloride (ZnCl_2), titanium chloride (TiCl_3), and uranyl nitrate ($\text{UO}_2(\text{NO}_3)_2$). All chemicals were purchased from Nevareaktiv LLC (Saint-Petersburg, Russia) at 99.9% purity without additional purification.

2.2. Synthesis Method

2.2.1. Co-Fe LDH Synthesis

For the synthesis, 18. mL of a 3.5 M NaOH solution was added to 100 mL of a 1 M Na_2CO_3 solution with vigorous stirring. A mixture containing 100 mL of $\text{FeCl}_3 \cdot 6\text{H}_2\text{O}$ with a concentration of 0.5 M and 100 mL of $\text{CoCl}_2 \cdot 6\text{H}_2\text{O}$ with a concentration of 1 M was added dropwise to the resulting solution. The concentrations of iron chloride and cobalt chloride in the solution obtained after mixing were 0.25 M and 0.5 M, respectively.

The pH values of the solution mixture were higher than 10 during the synthesis process. The resulting precipitate was filtered off, washed with distilled water, and dried at 100 °C for 6 h until excess moisture was completely removed. The dried materials were crushed, and a fraction with a grain size of 0.1–0.3 mm was selected. Before starting the experiment, the materials were additionally washed from dust particles by decanting distilled water.

2.2.2. Ni-Fe LDH Synthesis

The synthesis of Ni-Fe was carried out according to the method described above. The mixture containing 100 mL of $\text{FeCl}_3 \cdot 6\text{H}_2\text{O}$ with a concentration of 0.5 M and 100 mL of $\text{NiCl}_2 \cdot 6\text{H}_2\text{O}$ with a concentration of 1 M was used to precipitate Ni-Fe LDH. The concentrations of iron chloride and nickel chloride in the solution obtained after mixing were 0.25 M and 0.5 M, respectively.

2.2.3. Zn-Ti LDH Synthesis

The synthesis of Ni-Fe was carried out according to the method described above. The mixture containing 100 mL of ZnCl_2 with a concentration of 0.06 M and 100 mL of TiCl_3 with a concentration of 0.12 M was used to precipitate Zn-Ti LDH. The concentrations of titanium chloride and zinc chloride the solution obtained after mixing were 0.03 M and 0.06 M, respectively.

2.3. Characterization Methods

Identification of the crystalline phases of the obtained samples was carried out using X-ray diffraction analysis (XRD), $\text{CuK}\alpha$ radiation, Ni filter, average wavelength (λ) 1.5418 Å, shooting angle range 10–80°, scanning step 0.02°, spectral recording speed –5°/min., on a D8 Advance “Bruker-AXS” X-ray diffractometer (Mannheim, Germany).

Differential thermal analysis and thermogravimetric analysis (DTA-TG) were performed on a Shimadzu DTG-60H (Kyoto, Japan) derivatograph analyzer in air in a platinum crucible at a heating rate of 10 °C/min at a temperature of 20–1000 °C.

The texture characteristics of the obtained material were studied using the low-temperature nitrogen adsorption–desorption method on a Quantachrome Autosorb IQ instrument (Houston, TX, USA). The values of the specific surface area S_{BET} (m^2/g) were calculated from isotherms of low-temperature nitrogen adsorption using the single-point

BET method [29,30]. The pore size distributions in the studied materials were determined using the DFT method.

Images of the surface of the samples were obtained by scanning electron microscopy (SEM) on a CrossBeam 1540 XB “Carl Zeiss” (SEM, Berlin, Germany) device with an attachment for energy-dispersive microanalysis (EDS) “Bruker” (Bremen, Germany).

The residual concentration of the U(VI) in the solution was determined spectrophotometrically by the change in optical density (before and after sorption) on a UV mini-1240 Shimadzu device (Kyoto, Japan) at a wavelength of 656 nm [31].

2.4. Study of U(VI) Sorption on Obtained Materials

The study of the sorption properties of LDH toward uranyl ions was carried out in batch sorption mode in distilled water, seawater, and in solutions of competing ions.

2.4.1. Sorption of U(VI) from Distilled Water

The nature of the sorption process was assessed using sorption isotherms obtained using solutions of different concentrations of $\text{UO}_2(\text{NO}_3)_2$ in distilled water. The concentration of uranyl ions in the initial solutions varied from 30 to 150 mg/L. The pH value in the initial solutions of uranyl ions was maintained at a level of pH = 6 by manual adjustment.

A 10 mg sample of the sorbent was placed in an Eppendorf tube, and 10 mL of a solution of uranyl ions with a concentration of 30, 60, 90, 120, and 150 mg/L (S:L = 1:1000) was added. A series of test tubes were mounted on a vertical shaker and mixed at a speed of 20 rpm [32]. Sorption was carried out for 24 h. After that, the sorbent was separated from the solution, and the residual content of uranyl ions in the test solution was determined by spectrophotometry by the change in optical density (before and after sorption) in the presence of Arsenazo III at a wavelength of 656 nm.

2.4.2. Sorption of U(VI) from Seawater

The experiment was carried out according to the method described above. Sorption isotherms were obtained using solutions of different concentrations of $\text{UO}_2(\text{NO}_3)_2$ in seawater.

The seawater samples were taken in the Amur Bay (Primorskiy Krai, Russia). The salinity of the seawater samples was 30 g/L. The concentration of uranyl ions in the initial solutions ranged from 30 to 150 mg/L.

2.4.3. Sorption of U(VI) in Presence of Competing Ions

To assess the influence of competing ions in a solution on the efficiency of sorption extraction of uranyl ions, a series of solutions were prepared containing a given concentration of uranyl ions and several salts containing competing ions: Na_2CO_3 , Na_2SO_4 , KNO_3 , NaCl , K_3PO_4 , and NaHCO_3 . The concentration of uranyl ions was 100 mg/L, and the concentration of competing ions varied from 0.01 M to 0.1 M. The pH value of the original test solutions was equal to 6.

The effect of the concentration of competing ions on the sorption efficiency of samples was studied using carbonate and sulfate ions in the concentration range of 0.01–1 M and a uranyl ion content of 20 mg/L.

Sorption was carried out in batch sorption mode for 24 h, according to the method described above.

Based on the obtained experimental data, sorption efficiency indicators, including degree of purification, distribution coefficient (K_d), and sorption exchange capacity (SEC), were carried out.

The degree of purification (S, %) was calculated according to Formula (1):

$$S = \frac{C_0 - C_e}{C_0} \cdot 100\%, \quad (1)$$

where C_0 —initial concentration of ^{238}U in the solution, mg/L;

C_e —equilibrium concentration of ^{238}U in the solution, mg/L.

The distribution coefficient (K_d , mL/g) was calculated according to Formula (2):

$$K_d = \frac{C_0 - C_e}{C_e} \cdot \frac{V}{m}, \quad (2)$$

where C_0 —initial concentration of ^{238}U in the solution, mg/L;

C_e —equilibrium concentration of ^{238}U in the solution, mg/L;

V —volume of the liquid phase, mL;

m —mass of the sorbent, g.

The calculation of the sorption exchange capacity SEC (mg/g) was performed according to Formula (3):

$$\text{SEC} = (C_0 - C_e) \cdot \frac{V}{m}, \quad (3)$$

where C_0 —initial concentration of ^{238}U in the solution, mg/L;

C_e —equilibrium concentration of ^{238}U in the solution, mg/L;

V —volume of the liquid phase, L;

m —mass of the sorbent, g.

The nature of the sorption process was assessed based on sorption isotherms, which represent the dependence of the amount of adsorbed substance on the concentration of the solution at a constant temperature. When describing sorption isotherms, the following equations were used: Freundlich (4) and Langmuir (5) [31]:

$$q_e = K_f \cdot C_e^m, \quad (4)$$

where C_e —equilibrium concentration of ^{238}U in the solution, mmol/L;

K_f —Freundlich constant characterizes the relative adsorption capacity and represents the value of adsorption at an equilibrium concentration equal to one;

m —indicator of the heterogeneity of exchange centers, which characterizes the change in the heat of adsorption depending on the degree of their filling.

$$q_e = q_{\max} \frac{K_L \cdot C_e}{1 + K_L \cdot C_e}, \quad (5)$$

where q_{\max} —maximum sorption exchange capacity (mmol/g);

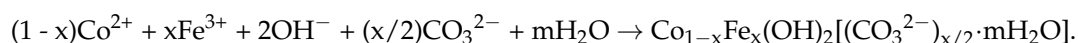
C_e —equilibrium concentration of ^{238}U in the solution, mmol/L;

K_L —adsorption equilibrium constant, which characterizes the adsorbent–adsorbate bond energy.

3. Results and Discussion

Sorption materials based on layered double hydroxides (Co-Fe LDH, Ni-Fe LDH, and Zn-Ti LDH) were synthesized using the direct coprecipitation method. The resulting samples are characterized by a solid powdery structure of irregular shape and brown, yellow, and white colors, respectively.

The mechanism for obtaining these compounds consists of coprecipitation from the solutions of salts of the corresponding di- and trivalent metals, followed by the crystallization and the formation of brucite-like layers with a uniform distribution of both metal cations and solvated interlayer anions. The synthesis of LDH can be schematically represented as follows:



According to the results of XRD analysis, it was revealed that the obtained samples have a well-crystallized phase structure, as evidenced by the presence of Bragg diffraction peaks in the X-ray diffraction patterns of the obtained materials (Figure 1).

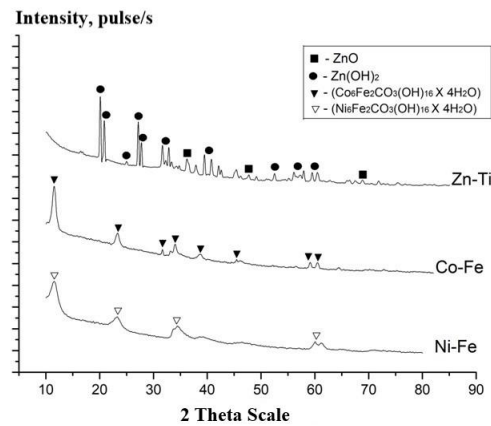


Figure 1. XRD patterns of obtained LDHs.

The phase composition of samples based on Co-Fe LDH and Ni-Fe LDH LDHs (Figure 1) corresponds to the well-known LDH formula $M^{2+}_{1-x}M^{3+}_x(OH)_2[A^{n-}]_x \cdot n \cdot mH_2O$, and the XRD pattern contains typical reflexes for this system.

It was revealed that the direct coprecipitation technique developed in this work is not suitable for the synthesis of Ti-Zn LDH since the actual composition of the claimed sample does not correspond to the expected one: the formation of not LDH but ZnO and $Zn(OH)_2$ phases is observed, which is probably due to the insufficient concentration of Ti^{3+} in the original solution.

The thermal stability of the studied samples was determined by thermal analysis. For all studied samples, the following patterns are observed on the TGA, DTA, and DTG curves (Figure 2): the low-temperature region corresponds to the removal of physically adsorbed water evaporation up to 150 °C; in the temperature range 200–250 °C the removal of interlayer water occurs; and the high-temperature region > 300 °C is attributed to the dehydroxylation of brucite-like layers and the removal of interlayer anions.

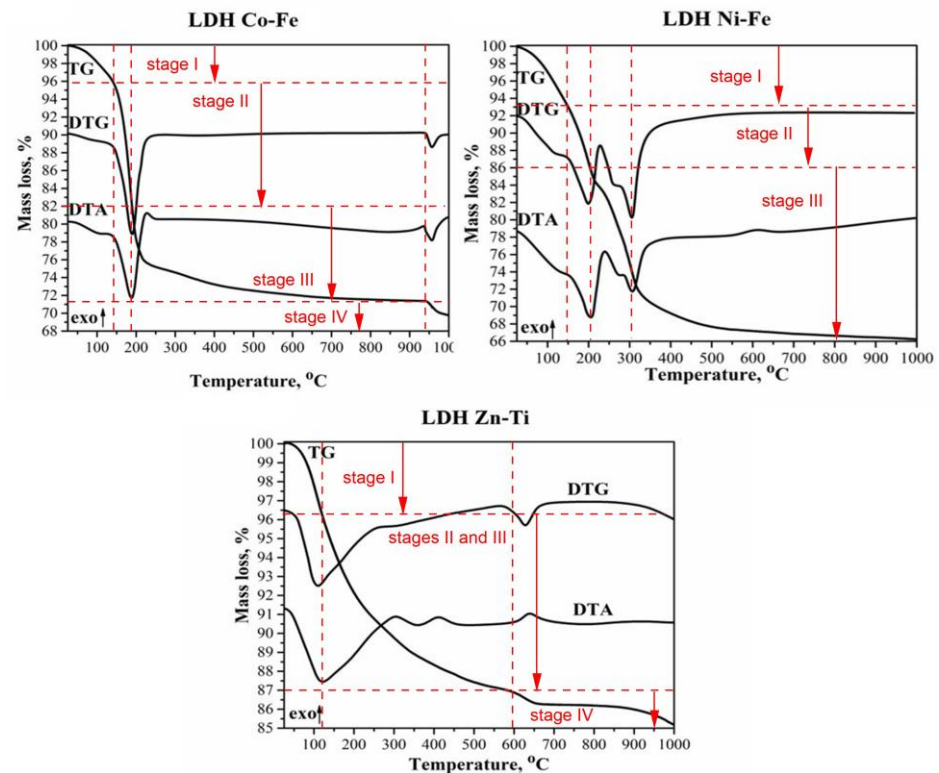


Figure 2. TGA, DTA, and DTG curves of obtained LDHs.

Thermal decomposition of the Co-Fe-LDH sample occurs in four clearly distinguishable stages (Figure 2). Stage I is associated with the evaporation of water adsorbed on the surface of the sample in the range from 20 to 140 °C (Table 1). With further heating to 190 °C, intercalated water evaporates, which corresponds to the occurrence of stage II. In the range from 190 to 940 °C, stage III occurs, associated with the final evaporation of intercalated water, dehydration of hydroxyl groups, and destruction of brucite-like layers. Upon reaching 940 °C, an endo-effect is observed associated with the decomposition of the formed carbonates. The decomposition of the Ni-Fe-LDH sample proceeds in a similar manner, but no clearly distinguishable stage IV is observed (Table 1). Since the phase composition of the Zn-Ti-LDH sample is different from Ni-Fe-LDH and Co-Fe-LDH, the shape of the DTA/TGA/DTG curves is also significantly different (Figure 2). Firstly, stage I, associated with the loss of adsorbed water, occurs up to a temperature of 120 °C. Stages II and III, associated mainly with the loss of intercalated water, as well as with the dehydration of hydroxyl groups, occur simultaneously in the range from 120 to 600 °C. Stage IV, associated with decarbonization, begins already at 600 °C. The observed patterns of the thermal destruction of synthesized LDHs coincide with the thermogravimetric data given in the literature [33–36].

Table 1. Thermogravimetric parameters of the obtained samples.

Sample	Stage (Temperature, °C)	Weight Loss, %	Total Weight Loss, %
Co-Fe-LDH	Stage I (20–140 °C)	4.1	30.2
	Stage II (140–190 °C)	13.9	
	Stage III (190–940 °C)	10.8	
	Stage IV (940–1000 °C)	1.4	
Ni-Fe-LDH	Stage I (20–150 °C)	6.8	33.7
	Stage II (150–205 °C)	7.2	
	Stage III (205–1000 °C)	19.7	
Zn-Ti-LDH	Stage I (20–120 °C)	3.7	14.8
	Stages II–III (120–600 °C)	9.3	
	Stage IV (600–1000 °C)	1.8	

Table 1 presents the thermogravimetric parameters of the obtained samples.

The isotherms of low-temperature nitrogen adsorption–desorption for the obtained materials under study (Figure 3) are of the IV type with a pronounced hysteresis loop, attributed to the process of capillary condensation in mesopores. A curved initial region indicates a strong adsorbate–adsorbent interaction. The specific surface area for the Ni-Fe LDH sample ($S_{\text{BET}} = 129.5 \text{ m}^2/\text{g}$) exceeds the similar value for other samples by two times.

According to DFT studies, the structure of all studied samples is represented by mesopores. The Ni-Fe and Zn-Ti LDH samples consist of mesopores with $d = 5 \text{ nm}$; the Ni-Fe LDH also contains a small amount of macropores with a size of $d > 50 \text{ nm}$. The diameter of the mesopores of Co-Fe LDH has a wide distribution in the range of 5–50 nm, and the presence of macropores in the structure of the sample is observed.

Based on SEM surface images (Figure 4) of the studied samples, it was established that the surface morphology of Co-Fe LDH and Ni-Fe LDH samples is characterized by a loose microstructure. The coprecipitation method achieves a low dispersion of materials, which is confirmed by the particle size, which does not exceed 10 microns. The particles of the Co-Fe LDH sample are plate-shaped grains, which are characteristic of the LDH structure [37]. The Zn-Ti LDH sample is distinguished by its monolithic surface structure, which is associated with the phase composition in which zinc hydroxide is present.

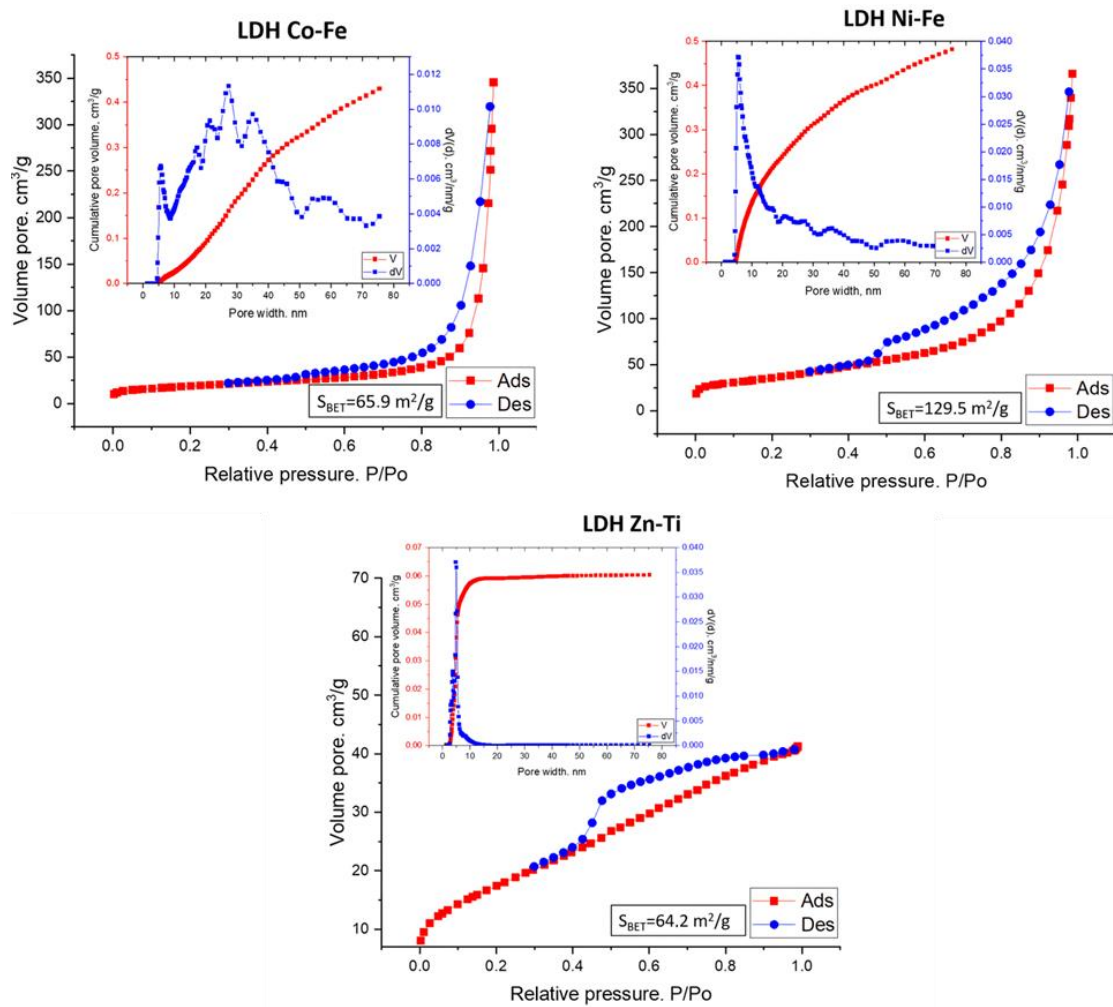


Figure 3. Isotherms of low-temperature nitrogen adsorption and DFT pore size distributions.

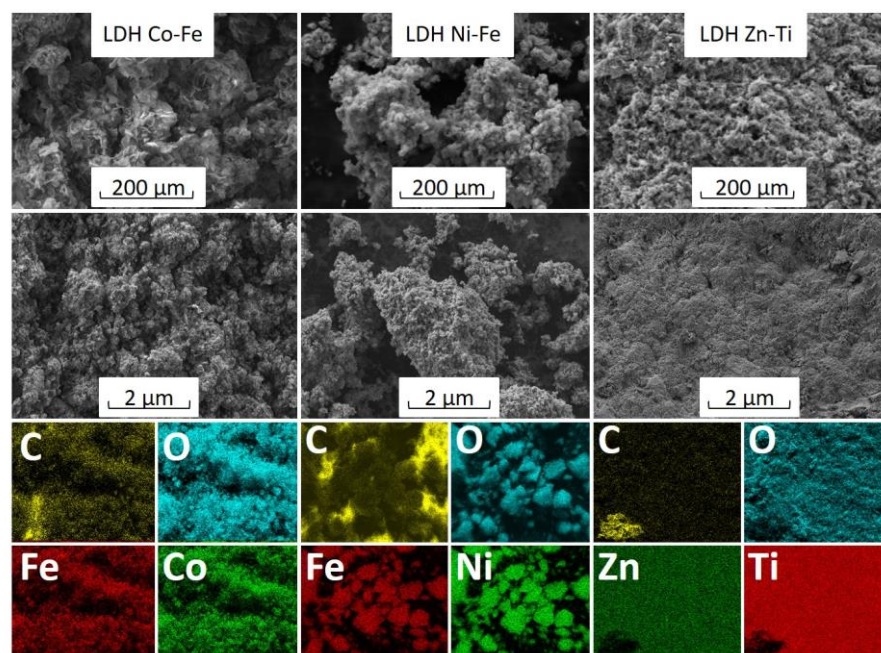


Figure 4. SEM images of the obtained LDHs' surfaces and EDS elemental distribution maps.

Using the EDS method, an image of the distribution of elements (Figure 4) on the surface of the samples and quantitative characteristics (Table 2) were obtained. It was revealed that the elemental composition of the surface is homogeneous and includes O, C, and Cl, and metals that form LDH: Fe, Co, Ni, Zn, and Ti.

Table 2. EDS elemental composition of obtained materials.

Sample	wt, %							
	C	O	Cl	Co	Fe	Ni	Zn	Ti
Co-Fe LDH	7.66	36.84	-	35.12	20.39	-	-	-
Ni-Fe LDH	-	48.21	0.49	-	15.3	36	-	-
Zn-Ti LDH	-	45.11	6.82	-	-	-	18.72	9.35

The results from EDS analysis correspond to the composition of the samples. The required quantitative ratio of metals for the formation of LDH Me^{2+}/Me^{3+} , approximately equal to 2:1, was observed for all studied samples. The obtained values for the mass fraction of elements were used to establish the general formula. The amount of intercalated water m was determined based on TGA data (mass loss in stage II corresponds mainly to the evaporation of intercalated water). Therefore, the general formula of the obtained Co-Fe-LDH is $[Co_{0.59}Fe_{0.36}(OH)_{1.9}](CO_3)_{0.18} \times 0.46H_2O$ and the obtained Ni-Fe-LDH general formula can be written as follows: $[Ni_{0.61}Fe_{0.27}(OH)_{1.76}](CO_3)_{0.14} \times 0.39H_2O$. The general formula of the resulting Zn-Ti-LDH cannot be determined from the analysis results since the diffraction patterns of this sample do not correspond to typical diffraction patterns of LDH. Therefore, the stoichiometric ratios in the general LDH formula do not describe the ratios of atoms in that sample.

The presence of chlorine in the obtained samples is associated with the inevitable intercalation of chloride ions, which occurs both due to their presence in the initial salts and due to the formation of the NaCl byproduct in the reaction mixture during the precipitation process. In the process of washing the resulting sediment from excess alkali, chloride ions are exchanged for carbonate ions, which enter distilled water through the absorption of atmospheric carbon dioxide. Accordingly, the concentration of chloride ions depends both on the intensity of washing and on the affinity of LDH for chloride and carbonate ions.

Regions containing many carbon atoms, as clearly visible from the SEM images (Figure 4), do not contain sorbent particles. In this regard, the different carbon content in the obtained samples does not indicate their different elemental composition. However, the provided SEM images show that the interlayer space of the LDH contains carbon in the form of carbonate ions, since dots corresponding to carbon atoms are also present on the sorbent particles. This is confirmed by the phase composition of the samples, since the diffraction patterns contain characteristic peaks of LDH in the carbonate form. The exact carbon content, however, cannot be determined by EDS.

The nature of the sorption process was assessed using sorption isotherms (Figure 5), obtained using solutions of different concentrations of $UO_2(NO_3)_2$ in distilled and seawater (Amur Bay, Vladivostok).

According to the classification of C. H. Giles [38], the sorption isotherms of uranyl ions (Figure 5) can be attributed to the H-type, which is distinguished by a vertical initial section, which is due to the high affinity of sorption centers for U(VI). The obtained isotherms are characterized by a clearly defined plateau, which indicates the achievement of adsorption equilibrium and the filling of all adsorption centers.

According to the literature [10–15], the adsorption of uranium at pH = 6, at the indicated concentrations, occurs by a mechanism that includes the stages of the formation of negatively charged uranyl complexes with the carbonate ions contained in the interlayer space ($UO_2(CO_3)_2^{2-}$), and the subsequent intercalation of those complexes in the LDH interlayer space. At higher pH values, precipitation of uranyl hydroxide $UO_2(NO_3)_2$ can occur on the surface of the LDH.

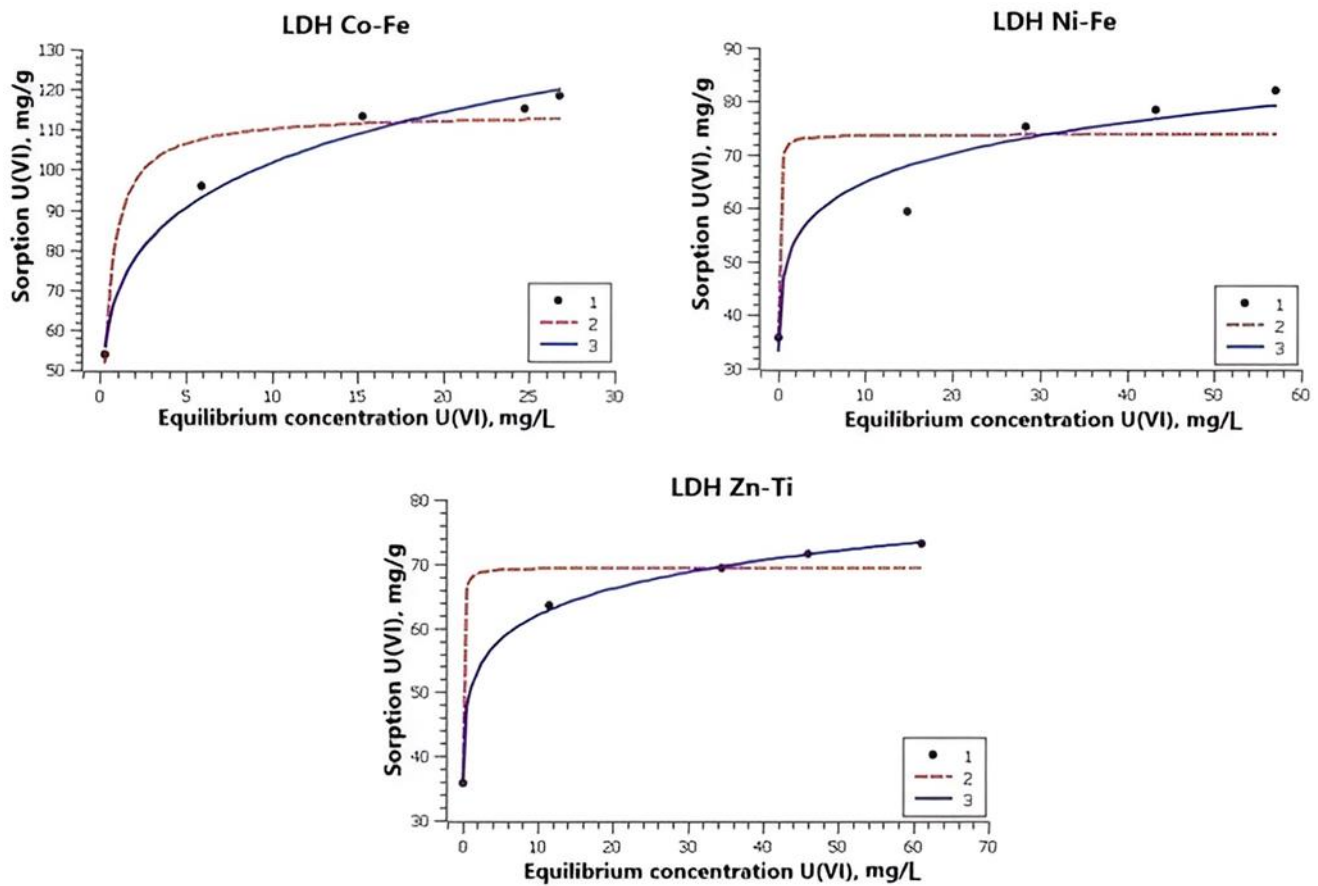


Figure 5. Isotherms of UO_2^{2+} adsorption from distilled water on obtained LDHs: (1) Experimental values approximation; (2) Using the Langmuir equation; (3) Using the Freundlich equation.

As shown in several studies [27,28], uranium can be desorbed using Na_2CO_3 (or $NaHCO_3$) treatment. In this case, there is no destruction of the crystalline structure of the sorbent, and desorption itself is carried out due to the exchange of substitution of complex uranium carbonate compounds contained in the interlayer space of the LDH with carbonate ions.

The obtained dependencies are reliably described by the Langmuir and Freundlich equations, as evidenced by the high values of the correlation coefficients (R^2). It was revealed that the highest value of the sorption exchange capacity (q_{max}) corresponds to the Co-Fe LDH sample (101.6 mg/g in seawater and 114.1 mg/g in distilled water). The Ni-Fe LDH and Zn-Ti LDH samples are significantly inferior in this value. The presence of various salts of seawater in the solutions and competing ions can reduce sorption efficiency by 10–40% (Figure 6).

Table 3 shows the parameters obtained by approximating experimental data using the Langmuir and Freundlich equations.

Figure 7 shows diagrams of the dependence of the distribution coefficient K_d (mL/g) of uranyl ions on the studied samples in distilled (Figure 7a) and seawater (Figure 7b) on the concentration of the initial solutions at a pH equal to 6.

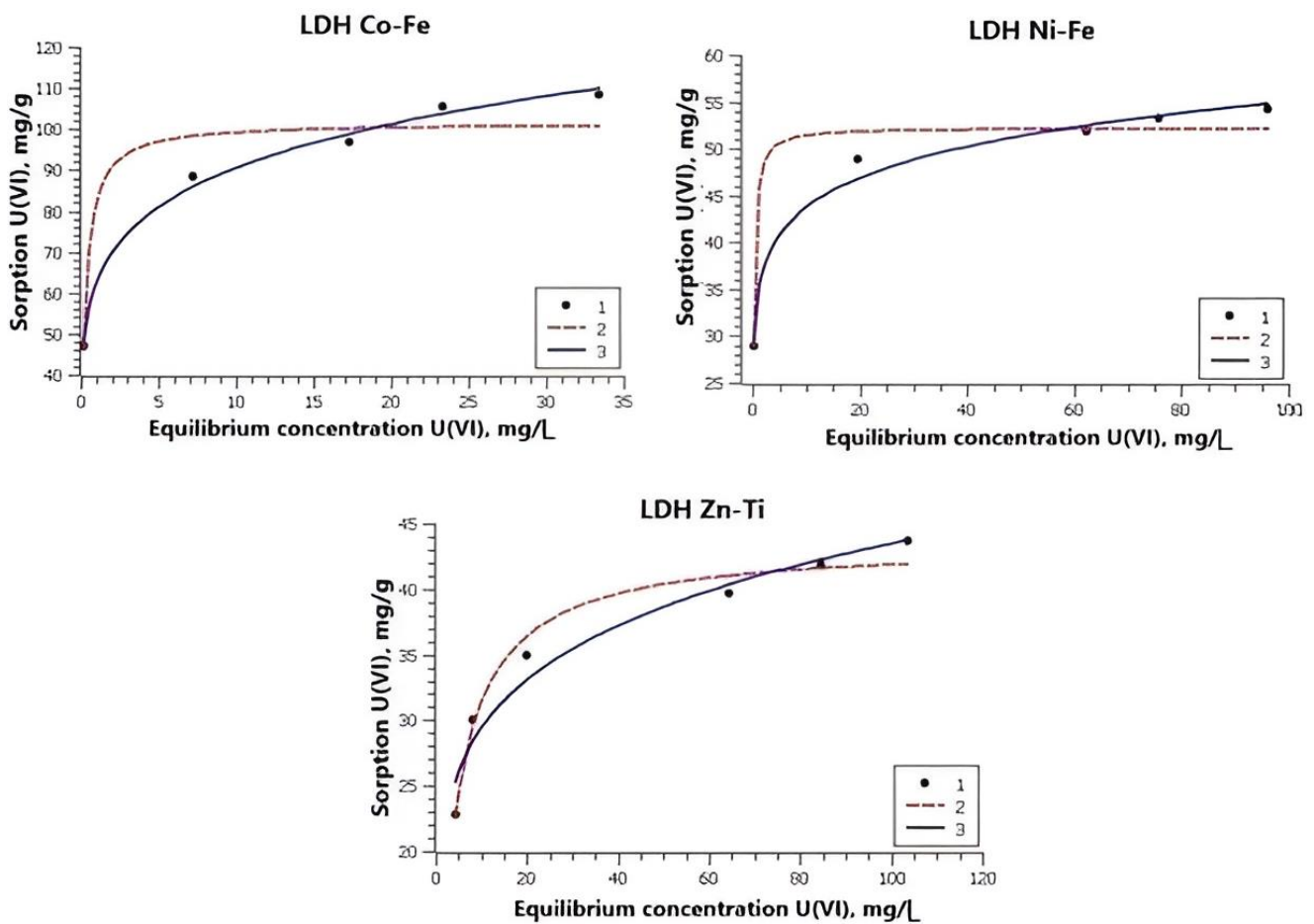


Figure 6. Isotherms of UO_2^{2+} adsorption from seawater on obtained LDHs (1) Experimental values approximation; (2) Using the Langmuir equation; (3) Using the Freundlich equation.

Table 3. Langmuir and Freundlich isotherm parameters for U(VI) adsorption on obtained LDHs.

Equation	Parameters	Co-Fe LDH		Ni-Fe LDH		Zn-Ti LDH	
		Seawater	Distilled Water	Seawater	Distilled Water	Seawater	Distilled Water
Freundlich	K_f	62.47 ± 1.79	68.91 ± 2.95	34.78 ± 0.97	49.80 ± 4.11	19.88 ± 1.53	49.96 ± 0.32
	n	0.16 ± 0.01	0.17 ± 0.01	0.10 ± 0.01	0.11 ± 0.02	0.17 ± 0.02	0.09
	R^2	0.99	0.98	0.98	0.94	0.956	0.99
Langmuir	q_{max}	10.60 ± 4.26	114.12 ± 4.34	51.85 ± 0.95	73.82 ± 4.97	43.51 ± 0.93	69.46 ± 2.10
	K_L	4.16 ± 1.41	2.78 ± 0.83	6.24 ± 1.06	31.27 ± 17.33	0.26 ± 0.03	35.2 ± 8.80
	R^2	0.92	0.94	0.96	0.80	0.976	0.94

Based on the calculated parameters of the sorption efficiency of the studied samples in relation to uranyl ions, it can be concluded that the Co-Fe LDH sample has a high sorption activity: the degree of extraction of uranyl ions reaches 99.9%, and the distribution coefficient K_d reaches 10^5 mL/g, which indicates its high selectivity for the extracted component.

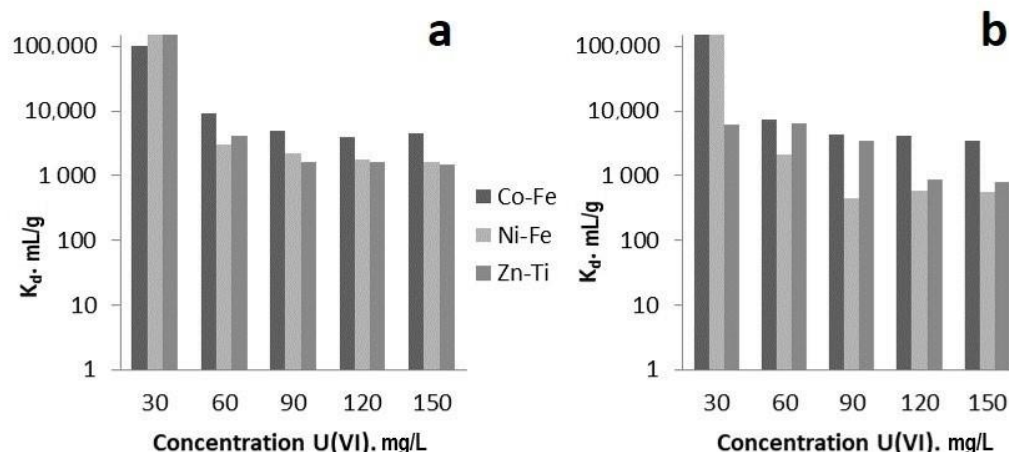


Figure 7. Distribution coefficient K_d in distilled water (a) and in seawater (b).

One of the key factors influencing the efficiency of sorption is the presence of competing and complexing ions in the solution. Ions form negatively charged stable complexes with uranium, which are sorbed to a limited extent on the surface of known sorbents and block their active centers [39]. Figure 8 shows the sorption efficiency indicators of the studied samples for uranyl ions in the presence of competing ions. The presented diagrams show that the lowest indicators of the degree of purification (S , %) and distribution coefficients K_d (mL/g) are registered in the solutions of Na_2CO_3 and NaHCO_3 because of the formation of uranyl-carbonate complexes [2,40]. However, the obtained values of the parameters are acceptable, which makes it possible to effectively use the materials under study for the extraction of uranyl ions from solutions with low salt content.

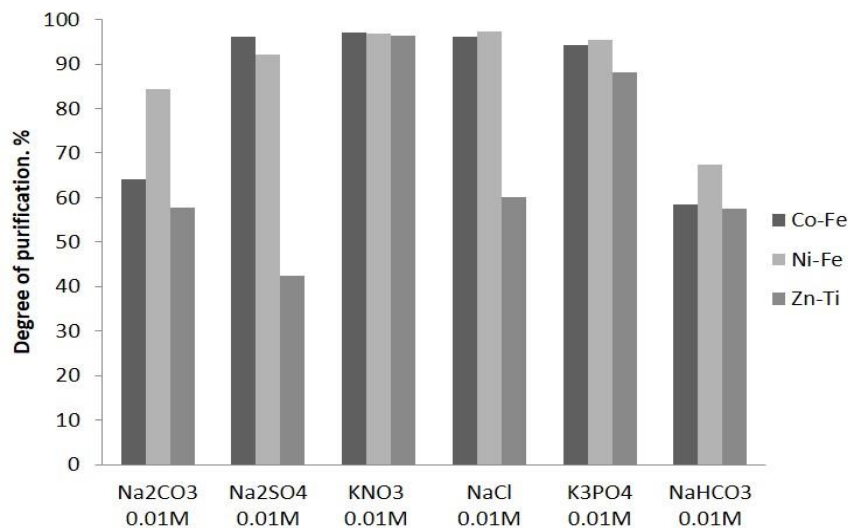


Figure 8. Degree of purification for U(VI) sorption in the presence of competing ions.

The effect of the concentration of carbonate and sulfate ions in solutions on the efficiency of sorption removal of U(VI) by the obtained materials was assessed based on the degree of purification at a pH value of 6 (Figure 9).

From the presented data, the increased content of the complexing agent significantly reduces the degree of purification of the studied solutions from uranyl ions; the presence of sulfate ions does not have such a significant effect.

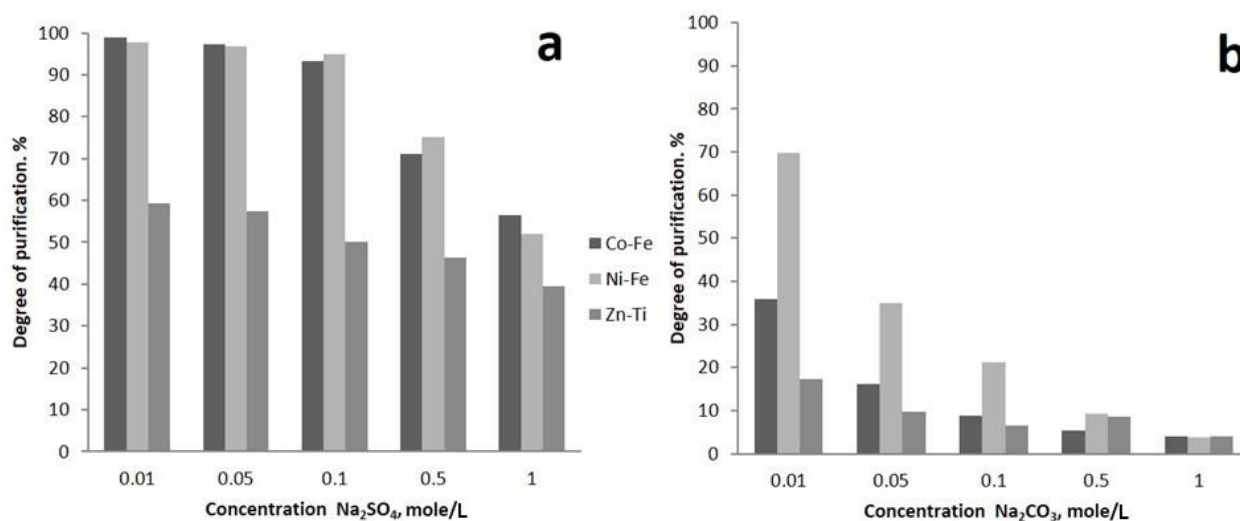


Figure 9. Degree of purification for U(VI) sorption in the presence of sulfate ions (a) and carbonate ions (b) with different concentrations of competing ions.

The Ni-Fe LDH sample has the highest rates of extraction of uranyl ions from salt solutions, which indicates the prospects for using this sample in solutions of similar composition.

4. Conclusions

The synthesis of sorption materials based on layered double hydroxides (Co-Fe LDH, Ni-Fe LDH, and Zn-Ti LDH) was carried out by a facile and environmentally friendly method of homogeneous coprecipitation. A high dispersion degree of the material and a low particle size of no more than 10 microns were achieved.

U(VI) adsorption on the obtained material from solutions, containing Na_2CO_3 , Na_2SO_4 , KNO_3 , NaCl , K_3PO_4 , and NaHCO_3 , was studied in batch mode. The degree of purification in the presence of these salts reached 99.9%, while the distribution coefficient K_d reached 10^5 mL/g. Sorption capacity q_{max} and equilibrium adsorption constants K_f and K_L for U(VI) adsorption in batch mode (for 24 h) from distilled and seawater were determined using the Freundlich and Langmuir equations. The highest sorption capacity of 101.6 mg/g in seawater and 114.1 mg/g in distilled water was registered for Co-Fe LDH. The presence of competing ions in seawater can reduce sorption efficiency by up to 40%. The high selectivity of the obtained materials is promising for industrial applications in uranium U(VI) capture.

The provided research allowed us to conclude that the obtained materials, Co-Fe LDH, Ni-Fe LDH, and Zn-Ti LDH are effective for the sorption removal of U(VI) from aqueous media of medium salinity.

Author Contributions: Conceptualization, V.A.B., A.N.D. and O.O.S.; Methodology, A.N.D., O.O.S., E.K.P., N.Y.S. and N.G.K.; Software, Z.C.K.; Validation, V.A.B. and N.P.I.; Formal analysis, A.N.D.; Investigation, V.A.B., A.N.D., A.I.I., E.K.P. and S.G.K.; Data curation, V.A.B., A.N.D., N.P.I., S.G.K. and E.K.P.; Writing—original draft, O.O.S., A.I.I. and E.K.P.; Writing—review & editing, A.N.D., N.Y.S. and N.G.K.; Project administration, E.K.P. and A.N.D.; Funding acquisition, E.K.P. and A.N.D.; All authors have read and agreed to the published version of the manuscript.

Funding: The study was financially supported within the State Assignment of the Ministry of Science and Higher Education of the Russian Federation, topic No. FZNS-2023-0003. The assessment of sorption properties was carried out with the financial support of the Russian Science Foundation (project 23-73-01160).

Data Availability Statement: The data presented in this study are available on request from the corresponding author.

Conflicts of Interest: The authors declare no conflict of interest.

References

1. Jiang, T.J.; Zhang, X.W.; Xie, C.; Wu, X.-Y.; Luo, C.-W.; Li, M.; Peng, Y. Effective capture of aqueous uranium using a novel magnetic goethite: Properties and mechanism. *J. Solid State Chem.* **2021**, *300*, 122236. [[CrossRef](#)]
2. Jana, A.; Unni, A.; Ravuru, S.S.; Das, A.; Das, D.; Biswas, S.; Sheshadri, H.; De, S. In-situ polymerization into the basal spacing of LDH for selective and enhanced uranium adsorption: A case study with real life uranium alkaline leach liquor. *Chem. Eng. J.* **2022**, *428*, 131180. [[CrossRef](#)]
3. Guo, X.; Ruan, Y.; Diao, Z.; Shih, K.; Su, M.; Song, G.; Chen, D.; Wang, S.; Kong, L. Environmental-friendly preparation of Ni–Co layered double hydroxide (LDH) hierarchical nanoarrays for efficient removing uranium (VI). *J. Clean. Prod.* **2021**, *308*, 127384. [[CrossRef](#)]
4. Yuan, X.; Jing, X.Y.; Xu, H.; Zhang, X.; Xu, J. Ni–Al layered double hydroxides modified sponge skeleton with polydopamine coating for enhanced U(VI) extraction from aqueous solution. *Chemosphere* **2022**, *287*, 131919. [[CrossRef](#)] [[PubMed](#)]
5. Chen, M.; Li, S.; Li, L.; Jiang, L.; Ahmed, Z.; Dang, Z.; Wu, P. Memory effect induced the enhancement of uranium (VI) immobilization on low-cost MgAl-double oxide: Mechanism insight and resources recovery. *J. Hazard. Mater.* **2021**, *401*, 123447. [[CrossRef](#)] [[PubMed](#)]
6. Nestroina, O.V.; Ryl'tsova, I.G.; Yapryntsev, M.N.; Lebedeva, O.E. Effect of the Synthesis Method on the Phase Composition and Magnetism of Layered Double Hydroxides. *Inorg. Mater.* **2020**, *56*, 747–753. [[CrossRef](#)]
7. Ebitani, K.; Motokura, K.; Mori, K.; Mizugaki, T.; Kaneda, K. Reconstructed hydrotalcite as a highly active heterogeneous base catalyst for carbon-carbon bond formations in the presence of water. *J. Org. Chem.* **2006**, *71*, 5440–5447. [[CrossRef](#)] [[PubMed](#)]
8. Pavel, O.D.; Birjega, R.; Che, M.; Costentin, G.; Angelescu, E.; Şerban, S. The activity of Mg/Al reconstructed hydrotalcites by “memory effect” in the cyanoethylation reaction. *Catal. Commun.* **2008**, *9*, 1974–1978. [[CrossRef](#)]
9. Li, Q.; Xing, L.; Lu, X.; Li, N.; Xu, M. Magnetic properties of Mg/Co(II)-Al/Fe(III) layered double hydroxides. *Inorg. Chem. Commun.* **2015**, *52*, 46–49. [[CrossRef](#)]
10. Bunney, K.G.; Cumberland, S.; Douglas, G. Mechanisms of Uranyl Sequestration by Hydrotalcite. *ACS Omega* **2017**, *2*, 7112–7119. [[CrossRef](#)]
11. Zou, Y.; Liu, Y.; Wang, X.; Sheng, G.; Wang, S.; Ai, Y.; Ji, Y.; Liu, Y.; Hayat, T.; Wang, X. Glycerol-Modified Binary Layered Double Hydroxide Nanocomposites for Uranium Immobilization via Extended X-ray Absorption Fine Structure Technique and Density Functional Theory Calculation. *ACS Sustain. Chem. Eng.* **2017**, *5*, 3583–3595. [[CrossRef](#)]
12. Linghu, W.; Yang, H.; Sun, Y.; Sheng, G.; Huang, Y. One-Pot Synthesis of LDH/GO Composites as Highly Effective Adsorbents for Decontamination of U(VI). *ACS Sustain. Chem. Eng.* **2017**, *5*, 5608–5616. [[CrossRef](#)]
13. Yang, L.; Qiao, B.; Zhang, S.; Yao, H.; Cai, Z.; Han, Y.; Li, C.; Li, Y.; Ma, S. Intercalation of salicylaldehyde into layered double hydroxide: Ultrafast and highly selective uptake of uranium from different water systems via versatile binding modes. *J. Colloid Interface Sci.* **2023**, *642*, 623–637. [[CrossRef](#)] [[PubMed](#)]
14. Zubair, M.; Ou, H.; Yang, Y.; Oldfield, D.T.; Thomsen, L.; Subhash, B.; Hamilton, J.L.; Wright, J.T.; Bedford, N.M.; Carolan, J.V. Enhanced uranium extraction selectivity from seawater using dopant engineered layered double hydroxides. *Energy Adv.* **2023**, *2*, 1134–1147. [[CrossRef](#)]
15. Foster, C.; Shaw, S.; Neill, T.S.; Bryan, N.; Sherriff, N.; Natrajan, L.S.; Wilson, H.; Lopez-Odrozola, L.; Rigby, B.; Haigh, S.J.; et al. Hydrotalcite Colloidal Stability and Interactions with Uranium(VI) at Neutral to Alkaline pH. *Langmuir* **2022**, *38*, 2576–2589. [[CrossRef](#)] [[PubMed](#)]
16. Pshinko, G.N. Layered double hydroxides as effective adsorbents for U(VI) and toxic heavy metals removal from aqueous media. *J. Chem.* **2013**, *2013*, 347178. [[CrossRef](#)]
17. Pshinko, G.N.; Puzyrnaya, L.N.; Shunkov, V.S.; Kosorukov, A.A.; Demchenko, V.Y. Removal of Radiocesium from Aqueous Media with Zinc–Aluminum Layered Double Hydroxide Intercalated with Copper(II) Hexacyanoferrate. *Radiochemistry* **2018**, *60*, 395–399. [[CrossRef](#)]
18. Keimirov, M.A. Sorbents with the structure of layered double hydroxides for aquatic media treatment from U(VI). *J. Water Chem. Technol.* **2016**, *38*, 128–133. [[CrossRef](#)]
19. Wang, X.; Yu, S.; Wu, Y.; Pang, H.; Yu, S.; Chen, Z.; Hou, J.; Alsaedi, A.; Hayat, T.; Wang, S. The synergistic elimination of uranium (VI) species from aqueous solution using bi-functional nanocomposite of carbon sphere and layered double hydroxide. *Chem. Eng. J.* **2018**, *342*, 321–330. [[CrossRef](#)]
20. Yuan, X.; Yin, C.; Zhang, Y.; Chen, Z.; Xu, Y.; Wang, J. Synthesis of C@Ni-Al LDH HSS for efficient U-entrapment from seawater. *Sci. Rep.* **2019**, *9*, 5807. [[CrossRef](#)]
21. Guo, Y.; Gong, Z.; Li, C.; Gao, B.; Li, P.; Wang, X.; Zhang, B.; Li, X. Efficient removal of uranium (VI) by 3D hierarchical Mg/Fe-LDH supported nanoscale hydroxyapatite: A synthetic experimental and mechanism studies. *Chem. Eng. J.* **2020**, *392*, 123682. [[CrossRef](#)]
22. Yang, Z.-Z.; Wei, J.-J.; Zeng, G.-M.; Zhang, H.-Q.; Tan, X.-F.; Ma, C.; Li, X.-C.; Li, Z.-H.; Zhang, C. A review on strategies to LDH-based materials to improve adsorption capacity and photoreduction efficiency for CO₂. *Coord. Chem. Rev.* **2019**, *386*, 154–182. [[CrossRef](#)]

23. Mei, H.; Tan, X.; Tan, L.; Meng, Y.; Chen, C.; Fang, M.; Wang, X. Retention of U(VI) by the Formation of Fe Precipitates from Oxidation of Fe(II). *ACS Earth Space Chem.* **2018**, *2*, 968–976. [[CrossRef](#)]
24. Pan, Z.; Li, W.; Fortner, J.D.; Giammar, D.E. Measurement and Surface Complexation Modeling of U(VI) Adsorption to Engineered Iron Oxide Nanoparticles. *Environ. Sci. Technol.* **2017**, *51*, 9219–9226. [[CrossRef](#)]
25. Scott, T.B.; Allen, G.C.; Heard, P.J.; Lewis, A.C.; Lee, D.F. The extraction of uranium from groundwaters on iron surfaces. *Proc. R. Soc. A Math. Phys. Eng. Sci.* **2005**, *461*, 1247–1259. [[CrossRef](#)]
26. Tan, L.; Wang, Y.; Liu, Q.; Wang, J.; Jing, X.; Liu, L.; Liu, J.; Song, D. Enhanced adsorption of uranium (VI) using a three-dimensional layered double hydroxide/graphene hybrid material. *Chem. Eng. J.* **2015**, *259*, 752–760. [[CrossRef](#)]
27. Li, S.; Wang, Y.; He, J.; Qiao, J.; Yang, Y.; Xiong, Z.; Wang, G. Adsorption of uranium (VI) by a MgAl-DHBDC/LDH composite: Kinetic, mechanistic and thermodynamic studies. *J. Radioanal. Nucl. Chem.* **2023**, *332*, 4255–4269. [[CrossRef](#)]
28. Yusheng, W.; Ying, D.; Wenmei, H.; Jinhua, X.; Qinqin, T. Uranium-specific adsorbent L-serine intercalated Mg-Al layered bimetallic (hydrogen) oxides for selectively treating uranium-containing wastewater. *J. Radioanal. Nucl. Chem.* **2023**, *332*, 3741–3752. [[CrossRef](#)]
29. Yarusova, S.B.; Shichalin, O.O.; Belov, A.A.; Azon, S.; Buravlev, I.Y.; Golub, A.; Mayorov, V.Y.; Gerasimenko, A.; Papynov, E.; Ivanets, A.; et al. Synthesis of amorphous KAlSi₃O₈ for cesium radionuclide immobilization into solid matrices using spark plasma sintering technique. *Ceram. Int.* **2022**, *48*, 3808–3817. [[CrossRef](#)]
30. Shichalin, O.O.; Papynov, E.K.; Nepomnyushchaya, V.A.; Ivanets, A.; Belov, A.; Dran'kov, A.; Yarusova, S.; Buravlev, I.; Tarabanova, A.; Fedorets, A.; et al. Hydrothermal synthesis and spark plasma sintering of NaY zeolite as solid-state matrices for cesium-137 immobilization. *J. Eur. Ceram. Soc.* **2022**, *42*, 3004–3014. [[CrossRef](#)]
31. Papynov, E.K.; Dran'kov, A.N.; Tkachenko, I.A.; Buravlev, I.Y.; Mayorov, V.Y.; Merkulov, E.B.; Fedorets, A.N.; Ognev, A.V.; Samardak, A.S.; Drenin, A.S.; et al. Synthesis and Sorption Characteristics of Magnetic Materials Based on Cobalt Oxides and Their Reduced Forms. *Russ. J. Inorg. Chem.* **2020**, *65*, 820–828. [[CrossRef](#)]
32. Dran'kov, A.; Shichalin, O.; Papynov, E.; Nomerovskii, A.; Mayorov, V.; Pechnikov, V.; Ivanets, A.; Buravlev, I.; Yarusova, S.; Zavjalov, A.; et al. Hydrothermal synthesis, structure and sorption performance to cesium and strontium ions of nanostructured magnetic zeolite composites. *Nucl. Eng. Technol.* **2022**, *54*, 1991–2003. [[CrossRef](#)]
33. María, A.A.; Yolanda, A.; Victoriano, B.; José, M.L.; José, M.M.; José, R.R.; Francisco, J.U. Thermal decomposition of Mg/Al and Mg/Ga layered-double hydroxides: A spectroscopic study. *J. Mater. Chem.* **1999**, *9*, 1603–1607.
34. Yang, W.; Kim, Y.; Liu, P.K.T.; Sahimi, M.; Tsotsis, T.T. A study by in situ techniques of the thermal evolution of the structure of a Mg-Al-CO₄ layered double hydroxide. *Chem. Eng. Sci.* **2002**, *57*, 2945–2953. [[CrossRef](#)]
35. Roelofs, J.C.A.A.; van Bokhoven, J.A.; van Dillen, A.J.; Geus, J.W.; Jong, K.P. The thermal decomposition of Mg-Al hydrotalcites: Effects of interlayer anions and characteristics of the final structure. *Chem.-A Eur. J.* **2002**, *8*, 5571–5579. [[CrossRef](#)]
36. Wei, G.; Liu, X.; Chen, S.; Shao, D.; Yuan, W.; Lu, X.; Xie, Y.; Shu, X. Direct immobilization of simulated nuclear waste in preformed Gd₂Zr₂O₇ pyrochlore via spark plasma sintering reaction. *Mater. Chem. Phys.* **2022**, *291*, 126711. [[CrossRef](#)]
37. Huang, Z.; Wu, P.; Gong, B.; Fang, Y.; Zhu, N. Fabrication and photocatalytic properties of a visible-light responsive nanohybrid based on self-assembly of carboxyl graphene and ZnAl layered double hydroxides. *J. Mater. Chem. A* **2014**, *2*, 5534–5540. [[CrossRef](#)]
38. Giles, C.N.; MacEwan, T.H.; Nakhwa, S.N.; Smith, D. Studies in adsorption. Part XI. A system of classification of solution adsorption isotherms, and its use in diagnosis of adsorption mechanisms and in measurement of specific surface areas of solids. *J. Chem. Soc.* **1960**, *786*, 3973–3993. [[CrossRef](#)]
39. Papynov, E.K.; Tkachenko, I.A.; Maiorov, V.Y.; Pechnikov, V.S.; Fedorets, A.N.; Portnyagin, A.S.; Dran'kov, A.N.; Buravlev, I.Y.; Grishin, A.V.; Tananaev, I.G.; et al. Nanostructured Magnetic Sorbents for Selective Recovery of Uranium(VI) from Aqueous Solutions. *Radiochemistry* **2019**, *61*, 28–36. [[CrossRef](#)]
40. Wang, Q.; Huang, J.; Ma, C.; Hu, H.; Shen, C.; He, S.; Li, P. Highly efficient and reusable Mg-Fe layered double hydroxides anchored in attapulgite for uranium uptake from wastewater. *Chemosphere* **2023**, *321*, 138055. [[CrossRef](#)]

Disclaimer/Publisher's Note: The statements, opinions and data contained in all publications are solely those of the individual author(s) and contributor(s) and not of MDPI and/or the editor(s). MDPI and/or the editor(s) disclaim responsibility for any injury to people or property resulting from any ideas, methods, instructions or products referred to in the content.